# An Optimized Control System for the Independent Control of the Inputs of the Doherty Power Amplifier

Pallav Kumar Sah [1] , Matthew Poulton [2], Hung Luyen [3] and Ifana Mahbub [1,*]

[1] Department of Electrical and Computer Engineering, The University of Texas at Dallas, Richardson, TX 75080, USA; pallav.sah@utdallas.edu
[2] Qorvo, Richardson, TX 75082, USA; matthew.poulton@qorvo.com
[3] Department of Electrical Engineering, University of North Texas, Denton, TX 76205, USA; hung.luyen@unt.edu
[*] Correspondence: ifana.mahbub@utdallas.edu

**Abstract:** This study presents a systematic design of an optimized drive signal control system for 2.5 GHz Doherty power amplifiers (DPAs). The designed system enables the analysis of the independent control of the amplitude and phase for the signals between the main and peak amplifiers of the DPA. The independent control of the signal is achieved by incorporating a variable attenuator (VA) and a variable phase shifter (VPS) in each of the two parallel paths of the DPA. This integration allows for driving varying power levels with an arbitrary phase difference between the individual parallel PAs for reduced control complexity and power consumption. The specific VA (Qorvo QPC6614) and VPS (Qorvo QPC2108) components are used for the test system to provide an amplitude attenuation range from 0.5 dB to 31.5 dB and a phase range from $0°$ to $360°$ at the intended operating frequency of 2.5 GHz, offering the benefit of characterizing the behavior of PAs for an extensive range of drive signals to optimize the output performance, such as PAE or the ACLR. For experimental validation, the designed drive signal control system is integrated with GaN PAs (Qorvo QPD0005—DUT) with a $P_{1dB}$ of 37.7 dBm. Each PA is preceded by a drive amplifier with a gain of 17.8 dB to boost the power fed into the PA. In this manuscript, we analyzed and compared the PAE of the DPA and parallel-connected PA for diverse input signals generated using a designed optimized control system.

**Keywords:** Doherty power amplifier (DPA); drive amplifier; variable attenuator; variable phase shifter; Wilkinson power splitter; signal control system; Doherty power combiner; quarter-wave transmission line; directional coupler; power-added efficiency (PAE); adjacent channel leakage ratio (ACLR)

## 1. Introduction

As contemporary wireless communication systems advance to accommodate higher data transmission speeds, the performance of power amplifiers becomes paramount. To satisfy the demanding data capacity requirements of various real-time applications, it is imperative to improve the power efficiency at reduced power levels. However, it is hard to satisfy the required maximum output power with a significant gain and a high $P_{1dB}$ compression point with just a single power amplifier. Wireless communication systems are implemented with complex modulation techniques, like code-division multiple access (CDMA), orthogonal frequency-division multiplexing (OFDM), and quadratic-amplitude modulation (QAM), which have a high peak-to-average power ratio (PAPR). Using these techniques forces PAs to use large back-off power, which drops the power efficiency. To overcome these drawbacks, a linear high-efficiency power amplifier, i.e., the Doherty power amplifier, can be designed, developed, and implemented to improve the overall power system performance [1]. The load-modulated DPA has always been proven for its high drain efficiency for the range of back-off saturated output power, with high efficiency and good linearity for just a simple structure that makes it possible to implement in base

stations, satellites, etc. The basic DPA contains two individual amplifiers and a combiner with a quarter-wave transmission line at the input of either amplifier, which provides the impedance inversion between the two parallel-connected amplifiers. This quarter-wavelength transmission line acts as an active load modulator, which modulates the output load of the peak amplifier at the same time as it contributes the output power of the DPA, and this leads to an increase in efficiency at backed-off power levels. The main amplifier operates as a conventional Class AB amplifier to maintain the linearity at the output [2,3]. The peak amplifier operates as a Class C amplifier, which turns on when the main amplifier reaches saturation [4]. The peak amplifier helps maximize the output power with the maintained constant drain voltage of the main amplifier. Now, to analyze and optimize the DPA in a repeatable and predictable way, a sophisticated PA control system needs to be established [5–11]. Components such as phase shifters and variable attenuators, along with directional couplers, power splitters, and drive amplifiers, are utilized for developing such control system circuitry [12,13]. Implementing a variable attenuator and a phase shifter at the input of the amplifier gives the benefit of varying the input amplitude and delay of the signal. Moreover, it helps obtain a wide range of control characterization for PAs to obtain the best performance. Previous studies indicate that DPAs have demonstrated impressive efficiency across a broad spectrum of output power levels. Past works used analog and digital control systems for regulating the inputs of the DPA where all the control components were fabricated on the same PCB, which restricts the use of the control system for the other amplifiers [14–18]. Moreover, previous approaches show that either the control system was integrated at the input of a power divider, which limits the control range for two parallel-connected PAs, or two different RF generators were used for the inputs of the parallel branch instead of using a power divider, increasing the chance of error for the mismatch between two signals.

In this paper, a novel control system able to integrate with any power amplifier configured in a parallel combination (like the DPA) using a single RF generator is presented. The presented control design has the following novelty. The implementation of a VA and VPS in each branch of the DPA configuration provides more flexibility to modify each input RF signal, irrespective of amplifier biasing. In turn, it improves the possibility of changing or pulling the impedance (load) seen through the source by controlling the magnitude and phase of the current in each branch. This can be further acknowledged by realizing the voltage and impedance relations for the traditional DPA, shown in Equations (1) and (2) and Figure 1. From Equations (1) and (2), it can be concluded that varying the magnitude and phase for $I_1$ and $I_2$ will improve the load pulling (changes $Z_{in}$). Therefore, this novel technique of using a VA and VPS enhances the load modulation of the DPA and hence improves the efficiency to 40.69% compared to the parallel-connected PA and individual PA for the same input.
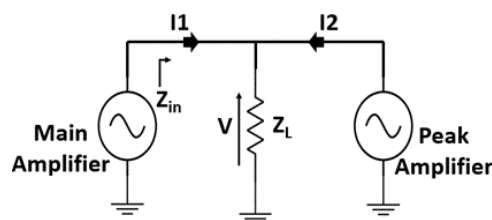


**Figure 1.** Impedance model for DPA.

$$V = Z_L(I_1 + I_2) \tag{1}$$

$$Z_{in} = Z_L\left(1 + \frac{I_2}{I_1}\right) \tag{2}$$

The implemented technique for the optimization of the DPA reduces the dependency on operating with fixed integrated amplifiers. It offers adaptability to configure the system

for a range of amplifiers with reduced complex circuits with a compact size and improved power consumption that is achieved when integrated with properly designed low-loss passive devices based on the theoretical line-budget analysis of the system. To address the uneven power distribution in both parallel branches of the system and to obtain precise magnitude ratios and phase differences for the two amplifiers, we used an AD8302 adapter to input the amplifiers. This will allow us to accurately measure the attenuation and phase shift of the input signal. This technique eliminates the chance of error in identifying the correct input for the characterization of the system, and this issue has not been addressed in previous works. A PA (Qorvo-QPD0005) of the exceptionally high output power of 37.7 dBm that corresponds to a 1 dB gain compression point with a maximum drain efficiency of 72.9% is used. The control system was created by combining a carefully optimized 20 dB directional coupler [19,20], a 3 dB power splitter [21–23], a quarter-wave transmission line [24], a Doherty power combiner, and various off-the-shelf components, including a GaN power amplifier [25,26], a drive amplifier [27,28], a VA, and a VPS [29–31].

This paper is organized as follows: Section 2 presents the system architecture of the designed and implemented optimized signal control system. Section 3 discusses the passive and active components used in the system, respectively. Section 4 presents the results and a discussion of the individual components used in the control system and the optimized configuration. Section 5 consists of the concluding remarks and future works.

## 2. System Architecture

The designed system is divided into three (3) sections: a designed control system, a parallel combination of power amplifiers, and instrument clusters (outputs). As mentioned before, two parallel methodologies of power amplifiers are used to plot the performance using the designed control system [32,33]. The first parallel combination PA is the Doherty power amplifier, which consists of two parallel-connected amplifiers operating with a fixed phase difference of 90° between their inputs, and their outputs are combined using the Doherty power combiner as shown Figure 2 and its corresponding test setup with the components used are shown in Figure 3. Moreover, the second PA configuration is the combination of the simple parallel-connected power amplifier operating in the phase and the same class of operation, with their outputs combined using a 3 dB Wilkinson power combiner. To independently control the inputs of both the amplifiers for both the DUTs, the control system is implemented, which controls the amplitude and phase of each input to obtain the optimized performance by characterizing the DUT. Independent amplitude control is achieved by integrating a variable attenuator in each branch, and then each output of the VA is independently phase-controlled by cascading with a VPS. Now, the output section involves the measuring instruments connected to the output of the DUT to measure the important parameters to draw the characteristics. The link-budget analysis is conducted for the 2.5 GHz operating frequency, taking into account the characteristics of the DUT. After integrating the control system with the DPA, the obtained estimated theoretical output is 28.1 dBm for a maximum attenuation of 31.5 dB, where for a minimum attenuation of 15 dB, the output is 40.2 dBm for a fixed input of 19 dBm. The VA, VPS, and drive amplifier were selected following the link-budget analysis discussed in our preliminary work [34] along with the corresponding model/manufacturer details, which can be found in the same. The power splitter, 20 dB directional coupler, and power combiner are fabricated on an FR4 substrate ($\varepsilon_r = 4.3$), which are incorporated into the overall control system. The architecture of the 3 dB Wilkinson power splitter, Doherty power combiner, and 20 dB directional coupler are discussed in Section 3.

To achieve the most effective output in a unified DPA architecture, precise adjustments in both the amplitude and phase variations must be configured. Usually, this is accomplished by manually tweaking the trace lines or by altering the surface-mount components. This is a complex and time-consuming methodology, which may compromise the final achieved performance. However, this designed control system enables independent control of the amplitudes and phases of the drive signals fed to the inputs of the two parallel

amplifiers used as the DPA architecture. Integrating both a VA and VPS in both parallel paths enables the adjustment of the power levels unevenly and applying arbitrary phase shifts to individual amplifiers. This configuration offers the advantage of evaluating the performance of the DUT when configured as a distributed power amplifier (DPA) across a wide spectrum of input signals. This assessment encompasses optimizing various output metrics, including the power-added efficiency, $P_{1dB}$ compression point, maximum output power, stability, gain, and adjacent channel leakage ratio (ACLR).
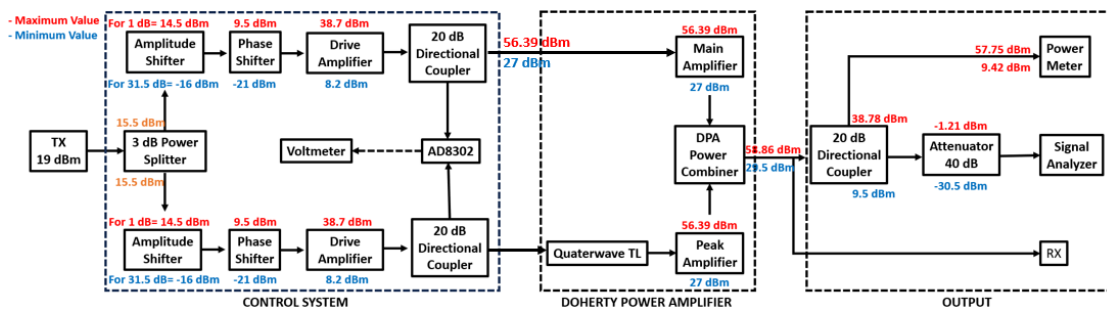


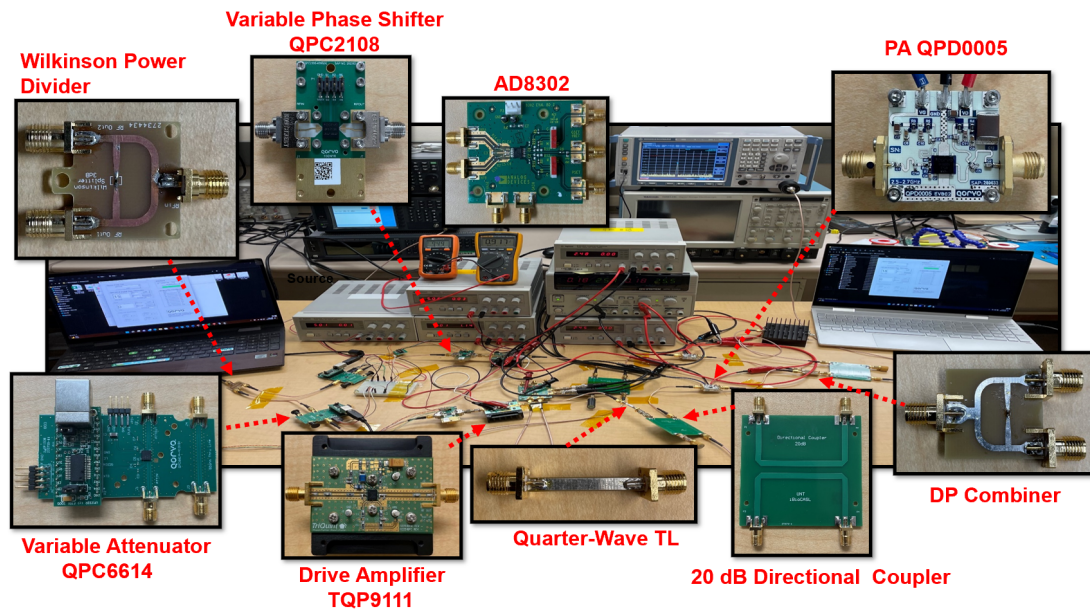**Figure 2.** Block diagram of optimized drive signal control system for DPA.



**Figure 3.** Control system for Doherty power amplifier.

## 3. Passive and Active Devices

### 3.1. The 3 dB Wilkinson Power Divider

The Wilkinson power divider plays a fundamental role in the construction of driver control circuitry. Instead of using two different RF generators for the parallel branch, this 2:1 Wilkinson power divider is used, reducing the chance of an amplitude and phase mismatch, which may arise due to the difference between signals generated by two different generators. The power splitter is created through the utilization of Keysight's Advanced Design System (ADS) automation software. In this design, FR4 is selected as the substrate material with a thickness of 1.2 mm, while copper with a thickness of 0.08 mm is chosen as the conductor material due to its excellent conductivity. Furthermore, the integration of a shunt resistor into the configuration serves to absorb the reflected power, consequently minimizing the insertion loss. The power ratio design methodology is employed to determine the shunt resistor's value, in conjunction with the dimensions (width and length) of the transmission lines. A comprehensive explanation of the procedure for computing line impedance and

shunt resistance in the context of the Wilkinson power splitter along with the corresponding width and length can be found in our previously published research [34].

### 3.2. Variable Attenuator

To achieve a wide range of inputs for the parallel-connected power amplifiers, a variable attenuator is employed in each branch of the inputs of the amplifiers. Variable attenuators are used to achieve a wide range of outputs for a given input signal, which is accomplished by attenuating the input signal. The used VA is a commercially available component (QPC6614) by Qorvo Inc., shown in Figure 3. This particular digital step variable attenuator is a 6-bit model, capable of delivering up to 31.5 dB of maximum attenuation, allowing for excellent linearity across a broad spectrum of input signals. Moreover, a VA is easy to control, as it can be either controlled by its GUI (Graphical User Interface) for different attenuations using a computer connected through a USB type-B, or it can also be controlled by an external bus according to the attenuation word truth table as shown in Table 1.

**Table 1.** Attenuation Word Truth Table.

| Attenuation Word | | | | | | |
|---|---|---|---|---|---|---|
| D5 (MSB) | D4 | D3 | D2 | D1 | D0 (LSB) | Attenuation State |
| H | H | H | H | H | H | 0 dB Ref. Insertion Loss |
| H | H | H | H | H | L | 0.5 dB |
| H | H | H | H | L | H | 1 dB |
| H | H | H | L | H | H | 2 dB |
| H | H | L | H | H | H | 4 dB |
| H | L | H | H | H | H | 8 dB |
| L | H | H | H | H | H | 16 dB |
| L | L | L | L | L | L | 31.5 dB |

Different attenuation ranges are selected based on the link-budget analysis for both the DUTs of the parallel combination of amplifiers. For the DUT, the Doherty power amplifier, the theoretical attenuation range is from 15 dB to 31.5 dB, whereas for the DUT, the parallel-connected amplifiers, the obtained range is from 22 dB to 31.5 dB. The long range of attenuation for the DPA is because of the introduction of quarter-wave transmission at the input of the peak amplifier, which introduces an insertion loss. Using this attenuation range, a wide range of inputs of amplifiers are obtained with the step size of 0.5 dB. The variable attenuator has a tolerance of 1.4 dB with an input $P_{0.1dB}$ of +30 dBm.

### 3.3. Variable Phase Shifter

Maintaining the purity of the phase and amplitude is a very challenging task, even when the outputs of the two parallel-connected amplifiers must be combined. To obtain a higher efficiency for the linear output, both output signals of the amplifiers should be combined with the correct phase. Thus, to control the delays of the output signal, the control system is equipped with two-phase shifters in both of the parallel branches following the VA. The variable phase shifter enables the control of the delays of each amplifier input signal generated by the VA, which in turn helps to combine the outputs with the correct phase for achieving higher efficiency. The phase shifters (Qorvo QPC2108) used in the control system are shown in Figure 3. This phase shifter has 360° coverage and offers an exceptional RMS phase error of <2.8° and an amplitude error of <0.4 dB over the entire operating frequency range of 2.5 to 4 GHz. It is a 6-bit variable digital phase shifter that can provide the maximum phase shifting of 360° with an LSB of 5.625° for an input $P_{1dB}$ of 23 dBm. The Qorvo QPC2108 is controlled by binary switching, for different phase shifts by applying 0/+5 V at the control switch, following the bias truth table as shown in Table 2.

**Table 2.** Bias Truth Table.

| | Bit Control | | | | | | |
|---|---|---|---|---|---|---|---|
| **Phase Shifter** | **5°** | **11°** | **22°** | **45°** | **90°** | **180°** | **REF** |
| 0° (REF) | 0 | 0 | 0 | 0 | 0 | 0 | 1 |
| 5° | 1 | 0 | 0 | 0 | 0 | 0 | 1 |
| 11° | 0 | 1 | 0 | 0 | 0 | 0 | 1 |
| 22° | 0 | 0 | 1 | 0 | 0 | 0 | 1 |
| 45° | 0 | 0 | 0 | 1 | 0 | 0 | 1 |
| 90° | 0 | 0 | 0 | 0 | 1 | 0 | 1 |
| 180° | 0 | 0 | 0 | 0 | 0 | 1 | 1 |
| 180° | 1 | 1 | 1 | 1 | 1 | 1 | 1 |

### 3.4. The 20 dB Directional Coupler

When implementing a parallel arrangement of amplifiers, the most significant challenge lies in accurately measuring the power signal. Moreover, to characterize the parallel combination of amplifiers, the input and output power levels need to be determined using a signal analyzer and power meter. As the system functions at a high-power level, expensive equipment with the ability to handle high-power signals is necessary for the analysis of these robust signals. To control the expanse, as shown in Figure 4b, a directional coupler with a coupling factor $C = 20$ is designed, which allows for maintaining a thorough connection in the circuit using Port 1 and Port 2, where the measuring instruments can be connected through Port 4, which is the 20 dB coupled port. The detailed design of the used 20 dB directional coupler is discussed in our prior published work [34]. To determine the dimensions of the microstrip coupled line for a frequency of 2.5 GHz, we employ Keysight's Advanced Design System (ADS) Linecalc tool.
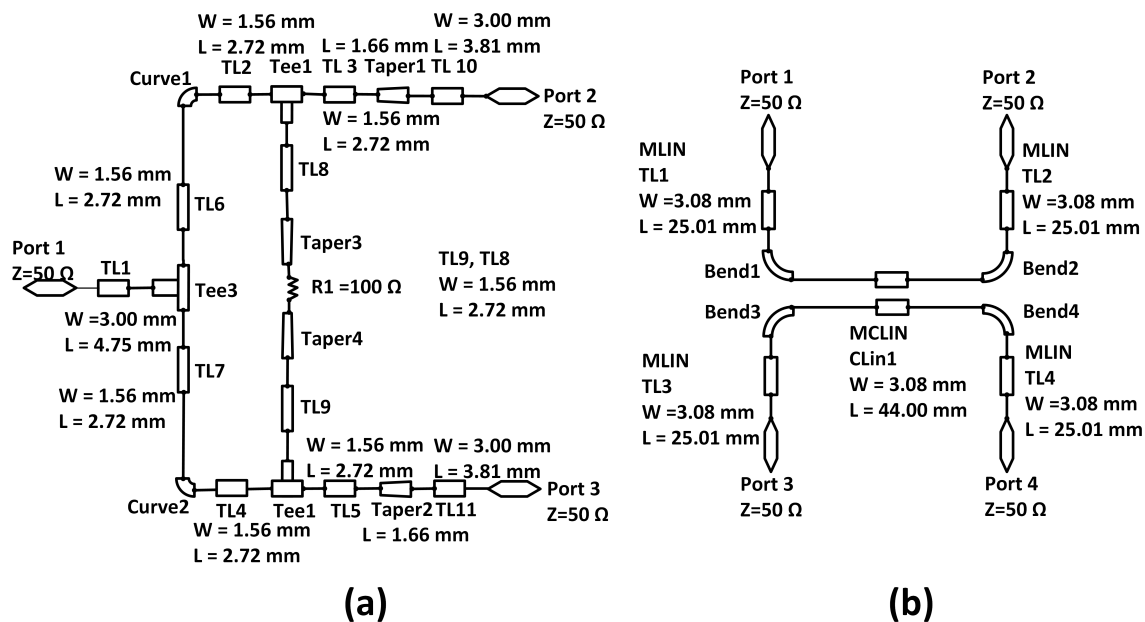


**Figure 4.** (**a**) Schematic of Wilkinson power splitter and (**b**) schematic of 20 dB directional coupler.

### 3.5. Doherty Power Combiner

For the designed Doherty power amplifier, the main amplifier is biased in the Class AB operation and the peak amplifier is biased in the Class C operation. To combine the outputs of these two amplifiers, an output-combining network called the Doherty power combiner is designed using transmission lines. The designed combiner combines the outputs of

the two parallel amplifiers biased in two different classes of operation. The combining network consists of a tuning circuit to bias the peak amplifier in the Class C operation. At the output of the main amplifier, a quarter-wavelength transmission line is employed to make the phases of both outputs equal at the recombination node, as shown in Figure 5b. The impedance of the transmission lines is obtained using the load-matching formula as shown in Equation (3), where $Z_{in}$ is the input impedance and $Z_l$ is the load impedance.
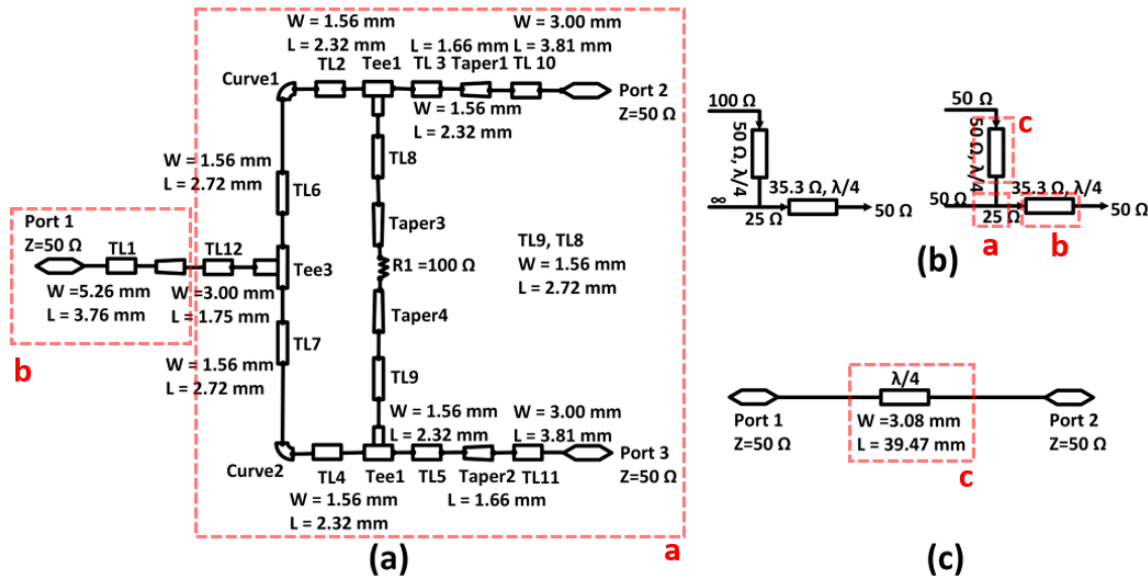


**Figure 5.** (**a**) Schematic of Doherty power combiner, (**b**) combining node, and (**c**) quarter-wavelength transmission line.

$$Z_0 = \sqrt{Z_{in} \times Z_l} \tag{3}$$

Figure 5b presents two cases. First is the initial case in which only the main amplifier is operating in the Class AB operation and the peak amplifier acts as an open circuit with infinite impedance, whereas the second case presents the impedances when the main amplifier saturates and the peak amplifier starts conducting at a high input power and sharing equal loads. The Doherty power combiner is designed and simulated using Keysight's Advanced Design System (ADS) [34]. The substrate material considered is FR4 with a thickness of 1.2 mm, and copper with a thickness of 0.2 mm is chosen as the conductor material due to its high conductivity. The microstrip line-based circuit (schematic) is shown in Figure 5a.

*3.6. Quarter-Wavelength Transmission Line*

In the DPA, the main amplifier operates in the Class AB mode, and the peaking amplifier operates in the Class C mode. At a high input power, the main amplifier reaches the state of saturation, and at that time, both amplifiers become active to deliver power to the load. The quarter-wavelength transmission ($\lambda/4$) line of characteristic impedance $Z_0 = 50 \, \Omega$ is chosen so that both the amplifiers provide the maximum power and efficiency by maintaining their optimum load impedance. The quarter-wavelength ($\lambda/4$) transmission line at the input of the peaking amplifier provides a delay of 90° to ensure the proper combination of the outputs of the two parallel-connected amplifiers at the combining node. This quarter-wavelength ($\lambda/4$) transmission line with a characteristic impedance of $Z_0 = 50 \, \Omega$ is designed and implemented using FR4 with a thickness of 2.2 mm, which is shown in Figure 5c, where, at the output of the main amplifier, a quarter-wavelength transformer recombines the output signal of the main and the peaking amplifiers. From this combining node of both PAs, the impedance is approximately half of the 50 $\Omega$ system impedance. Thus, a quarter-wavelength transformer is employed to convert the modulated

impedance to the system impedance, ensuring the maximum power transfer to the load is satisfied.

### 3.7. Power Amplifier (QPD0005)

Significant research endeavors have been conducted to assess and validate the technical potential of GaN HEMT. The requirement for robust equipment capable of operating effectively in challenging conditions, like for radio communication systems where temperature constraints are present, has led to the necessity of addressing reliability concerns [35]. The power amplifier used to implement this Doherty and parallel-connected amplifier structure is a commercial component, Qorvo QPD0005, as shown in Figure 3. It is a Gallium Nitride (GaN)-based power amplifier that is used for its increased power density, reliability, and gain in reduced size. Due to its reduced size and increased efficiency, this technology is employed in defense, aerospace, and much more complex applications, like phased arrays, radar, and base transceivers for 5G [36–38]. The QPD0005 operates in the frequency range from 2.5 to 5 GHz with a drain voltage equal to 48 V. It provides a gain of 18.8 dB for the input and output 1 dB compression points of 24 dBm and 37.7 dBm, respectively.

### 3.8. Drive Amplifier

Before feeding power to the amplifiers directly through the RF signal generator, the signal is passed through a control system that includes a power divider and then a VA and VPS for each branch. The presence of a power divider, VA, and VPS, which are all connected through RF cables, causes attenuation and insertion loss and reduces the input signal's power amplitude for the power amplifiers. To compensate for this loss, the input to the amplifier is boosted by implementing a drive amplifier before the main and the peak amplifiers. The drive amplifier (Qorvo TQP9111), as shown in Figure 3, is used as it is designed to boost its input signal, with a high gain of 29.2 dB at 2.5 GHz with a $P_{1dB}$ compression point of 32.5 dBm, which enables high linearity to drive and provide the maximum input to the power amplifier.

## 4. Measurements Results

The aim of this research is to design an optimized control system for the independent control of the inputs of the parallel combined power amplifiers to attain the highest PAE at the optimum input gain–power ratio and phase difference. The Wilkinson power divider, VA, VPS, and drive amplifier: all these instruments play a vital role in controlling the amplifier's input signal to achieve the highest PAE at the maximum output power. The designed control system is used for two different case scenarios: first for the Doherty power amplifier and second for the simple parallel-connected power amplifiers operating in the Class AB operation. The measured and simulated results for all the designed and fabricated components for the control system, including the power amplifiers, are presented in this section.

### 4.1. Wilkinson Power Divider

A Wilkinson power divider is designed to divide the total input power into two parallel branches. This Wilkinson power divider distributed the total input power for the control system into two equal halves to feed the main and peak amplifiers via other control instruments. Instead of using a power divider, two different RF generators can also be used, but this will increase the error of mismatch between two signals.

The S-parameters of the designed and fabricated Wilkinson power divider using FR4 with a thickness of 1.2 mm are shown in Figure 6. It can be seen from Figure 6a that the measured return losses for S22 and S33 are improved by 88.67% and 101.14%, but the measured insertion loss for S21 and S31 is increased by 7.14% in Figure 6b. The difference in the simulated and measured values is because of the real constraints, like to the occurrence of error, during fabrication and testing.
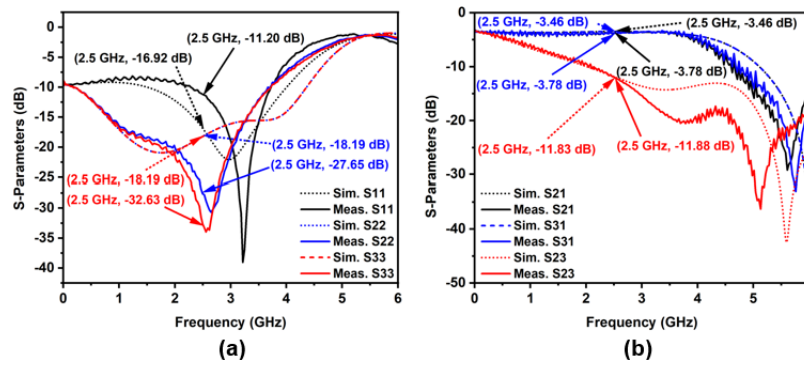
**Figure 6.** Wilkinson power divider: (**a**) return loss and (**b**) insertion and isolation loss.

### 4.2. Variable Phase Shifter

The variable phase shifter plays a vital role in the control system, which is employed in each branch to control the delay of the input signals of the amplifier. Controlling the delays of the input signals, in turn, controls the output signal and helps combine the output with the correct phase for higher PAE. The used VPS is a 6-bit variable digital phase shifter that gives coverage from 5° to 360°. The different phase shifts achieved and the errors at 2.5 GHz are shown in Table 3 and Figure 7a. The S-parameters are also obtained for the VPS; the insertion loss is 4.4 dB at 2.5 GHz as shown in Figure 7b.

**Table 3.** VPS phase shift and phase errors at 2.5 GHz.

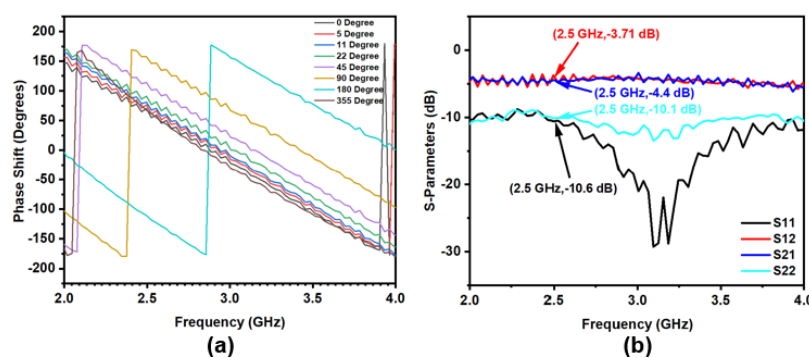| Given Phase Shift (Degrees) | Achieved Phase Shift (Degrees) | Phase Shift to Be Achieved (Degrees) | Error (%) |
|---|---|---|---|
| 0 | 70.22 (Reference) | 70.22 (Reference) | 0 |
| 5 | 76.44 | 75.22 | 1.62 |
| 11 | 80.96 | 81.22 | 0.32 |
| 22 | 91.10 | 92.22 | 1.21 |
| 45 | 114.22 | 115.22 | 0.86 |
| 90 | 157.61 | 160.22 | 1.62 |
| 180 | −110.49 | −109.78 | 0.64 |
| 355 | 67.32 | 65.22 | 3.21 |



**Figure 7.** Variable phase shifter's (**a**) phase shift and (**b**) S-parameters.

### 4.3. Drive Amplifier

As discussed above, the input signals must be boosted after passing through the power divider, VA, VPS, and RF cables as the input signal is attenuated due to their insertion loss. The drive amplifier (Qorvo TQP9111) used in this work that boosts the signal by 25.32 dB (S21) at 2.5 GHz to the input of the power amplifiers as the S-parameters is shown in Figure 8a. The obtained return losses for S11 and S22 are −14.6 dB and −10.02 dB,

respectively. The highest PAE achieved for the drive amplifier during the test is 23.2% at a maximum output of 30.55 dBm for an input of 10 dBm, which is calculated using Equation (4) and shown in Figure 8b. The actual gain, which is 28.8 dB, is 13.74% greater than the measured value.
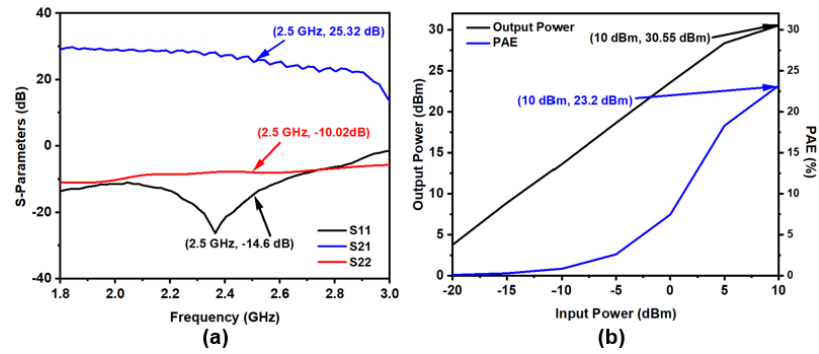


**Figure 8.** Drive amplifier: (**a**) S-parameters and (**b**) PAE and maximum output power.

$$PAE = 100 \times \frac{RF_{Pout} - RF_{Pin}}{P_{dc}} \qquad (4)$$

### 4.4. Power Amplifier (QPD0005)

The Gallium Nitride transistor—Qorvo QPD0005—PA is used to design the DUTs: first, the Doherty power amplifier, and second, the parallel-connected amplifiers. The Gallium Nitride transistor is selected because it provides higher efficiency with a minimal size, making it useful for most applications, like satellites, communication, robotics, etc. All the calculations and the link-budget analysis are performed based on the selected PA's gain, input, and output P1dB; compression point; and supply voltage. The S-parameters for the PA are shown in Figure 9a. The obtained input return loss is $-13.61$ dB, and the output return loss is $-5.5$ dB, where the measured gain is 17.43 dB at 2.5 GHz, which is 33.92% lower than the actual gain. The achieved higher efficiency is 36.54% at the maximum output of 34 dBm for the 20 dBm input. The plot for the PAE is shown in Figure 9b.
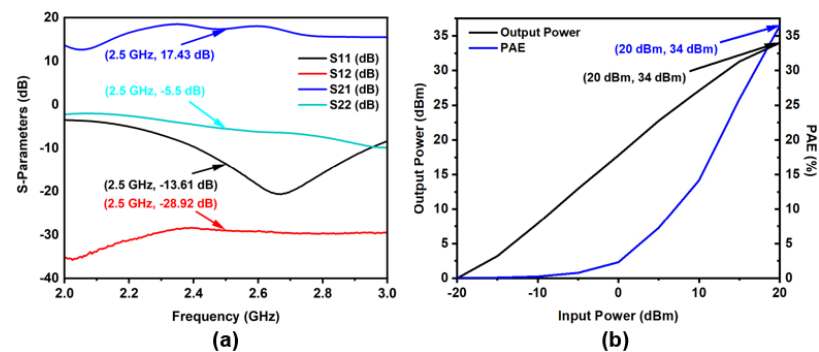


**Figure 9.** QPD0005: (**a**) S-parameters and (**b**) PAE and maximum output.

### 4.5. Quarter-Wavelength Transmission Line

To provide the input phase difference of 90° between the two parallel-connected amplifiers in the Doherty form, a designed quarter-wavelength transmission line is used with characteristic impedance, $Z_0 = 50$ Ω. The measured insertion loss is 1.44 dB, whereas the simulated insertion loss is 0.55 dB, as shown in Figure 10. This employed quarter-wave transmission line is supposed to provide a 90° phase shift, but during the test, it is noticed that it is providing a phase shift of $-110°$. As the designed quarter-wavelength transmission line provides the phase shift of $-110°$, the whole experiment for the DPA is performed accordingly, maintaining the phase gap of $-90°$ with the help of an integrated VPS in each parallel line providing an additional phase shift of $+20°$.
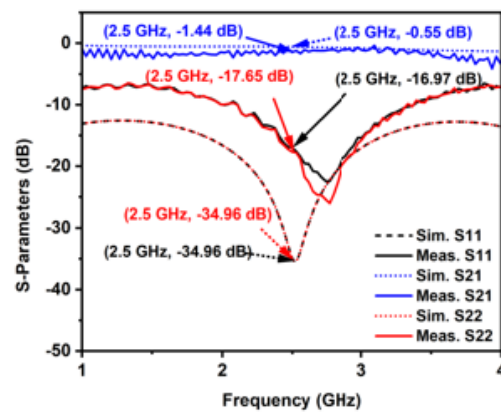
**Figure 10.** Return and insertion loss for quarter-wave TL.

### 4.6. Doherty Power Combiner

For the Doherty power amplifier, the main and peak amplifier inputs are 90° out of phase. Before combining the output of the amplifier, the phase shift needs to be eliminated. Therefore, a quarter-wave transmission line of 50 $\Omega$ is employed at the output of the main amplifier, compensating for the input phase difference in the PAs.

The return losses S11, S22, and S33 and the insertion losses S21 and S31 of the designed and fabricated Doherty power combiner using the FR4 dielectric substrate with a constant of 4.3 and thickness of 1.2 mm are shown in Figure 11a,b, respectively. It can be observed from Figure 11a that the measured return losses S11, S22, and S33 are −18.12 dB, −19.22 dB, and −19.61 dB, respectively, reduced from the simulated values, which are −16.91, −13.92, and −13.91, whereas the measured and simulated insertion losses S21 and S31 are approximately similar, equal to 0.5 dB, as shown in Figure 11b.
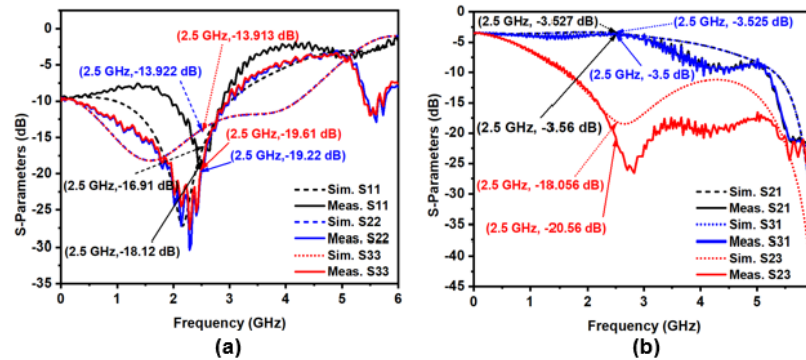


**Figure 11.** Doherty power combiner: (**a**) return loss and (**b**) insertion loss.

### 4.7. The 20 dB Directional Coupler

To characterize the DUTs, the inputs, outputs, gain, phase, and power need to be determined. Moreover, to connect the measuring instruments in the RF circuit, a 20 dB directional coupler is designed and fabricated on FR4. The measuring instruments are connected using Port 4, a 20 dB coupled port. The measured insertion loss, S41, is 0.08 dB, which is improved by 3.92% compared to the simulated loss, where the insertion loss, S21, i.e., through the port, remains the same and equals 1.11 dB, shown in Figure 12c. However, the return losses S11, S33, and S44 are improved compared to the simulated values, as shown in Figure 12a,b.
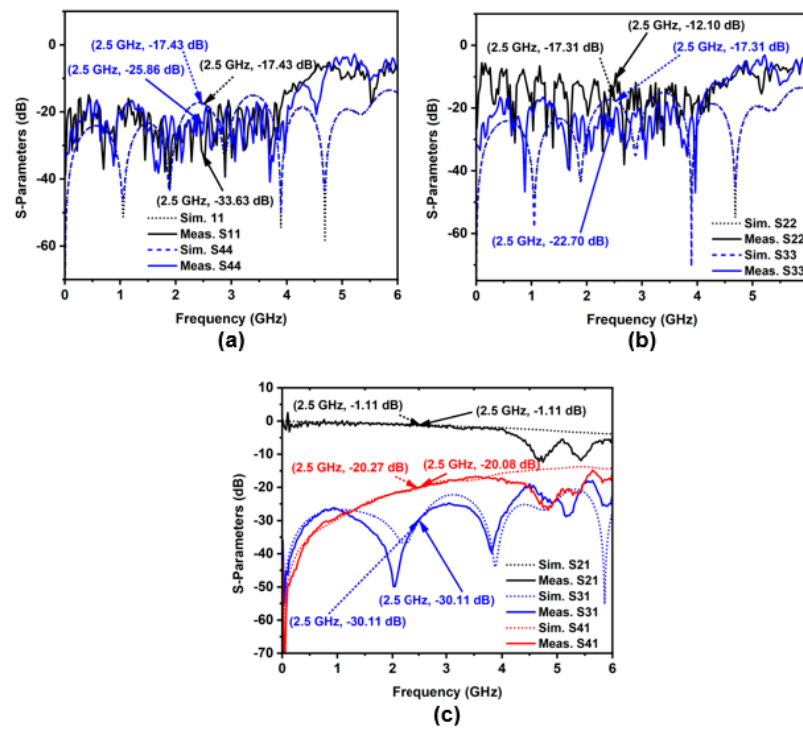
**Figure 12.** The 20 dB directional coupler: (**a**,**b**) return losses and (**c**) insertion losses.

*4.8. Enhanced Outputs for Optimized Inputs of the Designed System*

The presented research has showcased the improved performance of the DPA and parallel-connected power amplifiers by employing the designed control system. This system offers greater flexibility to individually adjust the input RF signal for each branch, leading to enhanced performance and optimized parameters, regardless of amplifier biasing. Consequently, it contributes to the refinement of the load pulling by enabling precise control of the current magnitude and phase in each branch. To achieve higher PAE for the most appropriate input gain ratio and the phase difference for the parallel combined power amplifiers considering two different DUTs, the measurements for both the DUTs show that a parallel combination of amplifiers enables the achievement of higher efficiency when the input gain ratio is zero and the phase difference between both inputs is close to zero as shown in Figures 13 and 14. It implies that higher PAE can be achieved when the outputs of the amplifiers are combined in the same phase.

For the first DUT, the Doherty power amplifier, a quarter-wavelength transmission line is employed at the input of the peak amplifier and another one at the output of the main amplifier to maintain the same phase while combining the outputs. This employed quarter-wave transmission line gives the measured phase shift of $-110°$ as discussed earlier. As a result, the highest PAE obtained is 40.67% at a maximum output power of 40.40 dBm for an input amplitude difference equal to 0 dB and an input phase difference of $-110°$, without phase correction for the quarter-wave transmission line as shown in Figure 13a,b. So, the maximum PAE and output are obtained at an input phase difference of $-110°$ because of the quarter-wavelength transmission line employed at the input of the peak amplifier. Similarly, in the case of parallel-connected PAs, the maximum PAE achieved is 32.70% at the maximum output power of 38.30 dBm for an input gain ratio of 0 dB and a phase difference of $0°$, shown in Figure 14. Based on the measurement observations discussed earlier for the DPA and parallel-connected PA, it can be inferred that enhanced results are attained by combining the amplifier outputs at the desired magnitude and phase control. This is accomplished by managing the system-optimized input through VA and VPS control.
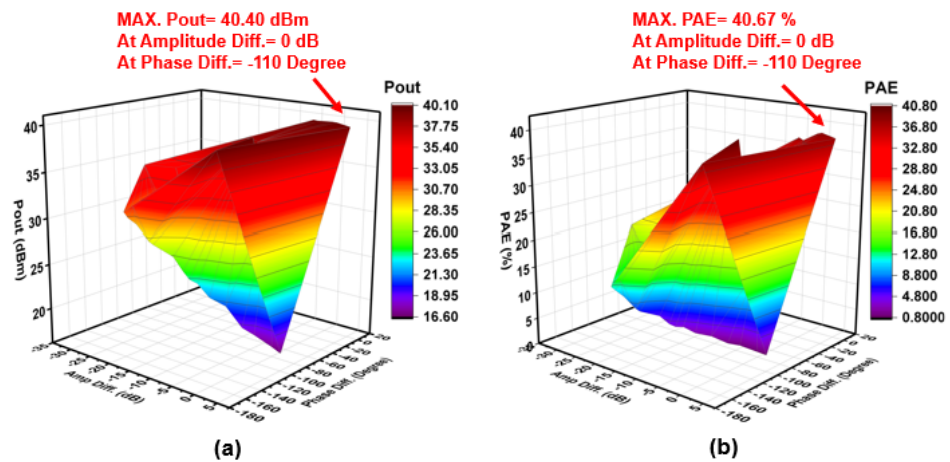
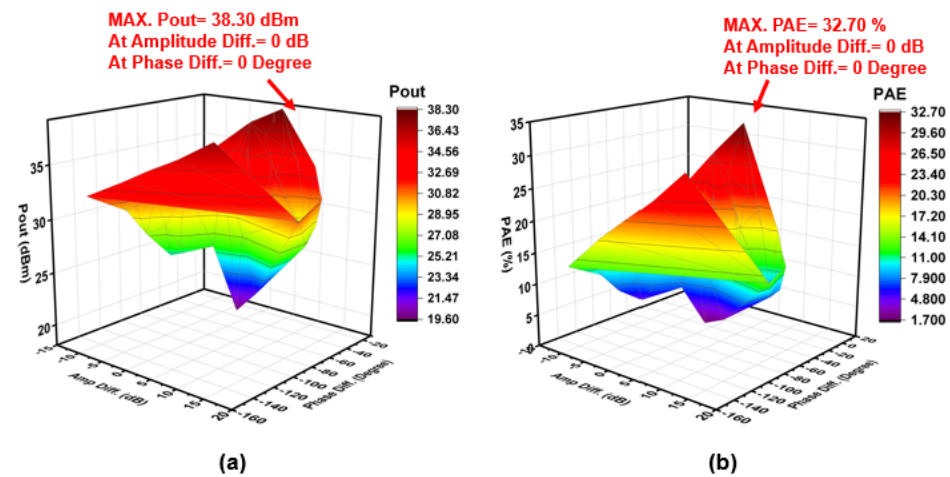**Figure 13.** Doherty power amplifier: (**a**) max. pout and (**b**) max. PAE.



**Figure 14.** Parallel-connected power amplifier: (**a**) max. pout and (**b**) max. PAE.

A comparison with the prior work is shown in Table 4 with the results obtained from this work. This manuscript's comparisons are established by considering the control systems' technique and performance, focusing on improving the DPA, regardless of the amplifiers and other devices employed. In the prior works [35,39,40], the system is designed for fixed PAs, which does not give the flexibility of characterizing the other amplifiers. In both the previous studies and the current work, the inputs and outputs are different due to the integration of distinct control systems with varying amplifier types, each with its unique biasing prerequisites. Unlike the previous research, the system we introduced features an innovative control system design that can seamlessly interface with a variety of power amplifiers. To demonstrate this, we tested it with a GaN power amplifier (Qorvo-QPD0005) as the Device Under Test (DUT), confirming its adaptability. Furthermore, the previous works for the designed DPA with all the components integrated on a single board resulted in a lower overall system efficiency compared to the work presented in this manuscript. The designed system also provides the benefit of identifying the actual input gain ratio and the phase difference of two parallel amplifiers by using a gain and phase detector (AD8302), connected just at the input of the PAs. In [39], two different RF generators are used to control the input amplitude and phase of amplifiers, which increases the chance of a mismatch error between two signals.

**Table 4.** Comparison with other works.

|  | Frequency (GHz) | Methods | PAE (%) | Type |
|---|---|---|---|---|
| [40] | 3.1 | Analog | 35.0 | DPA |
| [39] | 3.1 | Digital | 38.0 | DPA |
| [35] | 17.3–20.3 GHz | Analog | >35% | DPA |
| This Work | 2.5 | Digital | 36.62 | Parallel-Connected PA |
| This Work | 2.5 | Digital | 40.69 | DPA |

## 5. Discussion

In this article, an optimized drive signal control system for a parallel combination of power amplifiers at 2.5 GHz is presented. The integrated controlling blocks used in the designed system are analyzed by performing the link-budget analysis for a minimum/maximum input power of −16/14.5 dBm, respectively. With the design of the control system, the fabricated Wilkinson power splitter, Doherty power combiner, quarter-wave transmission line, and 20 dB directional coupler are individually configured with a lower insertion loss. A prototype for the effective control system is fabricated and measured. The fabricated control system modulates the divided input signal amplitude by attenuating it for the range of 1 dB to 31.5 dB at the step size of 0.5 dB and the varying phase from 0° to 180°, providing a wide range of input combinations to analyze the parallel-connected power amplifier and Doherty power amplifier.

Using the presented control system, the DPA and parallel-connected amplifiers are analyzed for equal/unequal input powers along with the same/unlike phases for each signal on account of an integrated VA and phase shifter in each parallel line. The measured realized PAE for the DPA is 40.69%, which is higher than the achieved PAE for parallel-connected amplifiers, i.e., 32.62% for the same inputs of the PA, provided in Figure 15. In contrast, it is obtained that for the measured system, the DPA achieved the maximum PAE when the input amplitude and phase differences are 0 dB and −110 degrees, respectively. Therefore, the proposed control system for DPA and parallel-connected amplifiers integrated with a VA and VPS improves the load modulation for the compact size and improved power consumption.
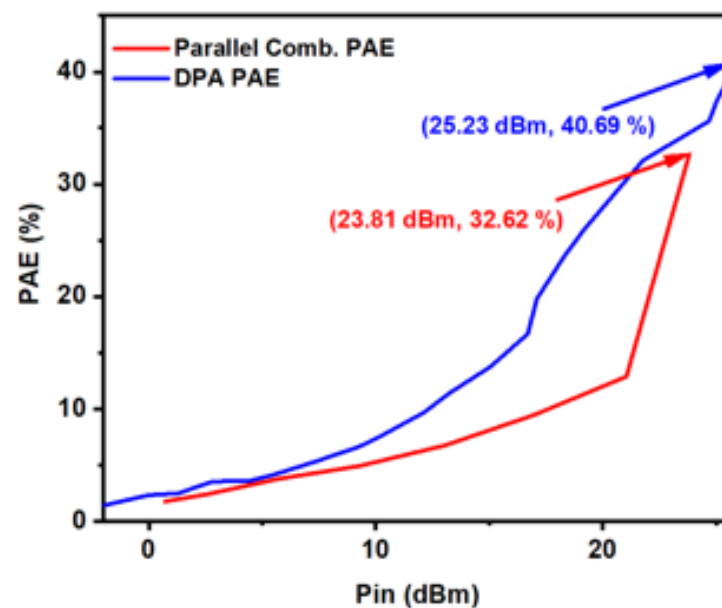


**Figure 15.** PAE for DPA and parallel PA.

# References

1. Camarchia , V.; Pirola, M.; Quaglia, R.; Jee, S.; Cho, Y.; Kim, B. The Doherty Power Amplifier: Review of Recent Solutions and Trends. *IEEE Trans. Microw. Theory Tech.* **2015**, *63*, 559–571. [CrossRef]
2. Raab, F.; Asbeck, P.; Cripps, S.; Kenington, P.; Popovic, Z.; Pothecary, N.; Sevic, J.; Sokal, N. Power amplifiers and transmitters for RF and microwave. *IEEE Trans. Microw. Theory Tech.* **2002**, *50*, 814–826. [CrossRef]
3. Kotzebue, K. A Quasi-Linear Approach to the Design of Microwave Transistor Power Amplifiers (Short Papers). *IEEE Trans. Microw. Theory Tech.* **1976**, *24*, 975–978. [CrossRef]
4. Holmes, D.G. A simple output impedance model for Doherty peaking sub-amplifiers biased in Class C. In Proceedings of the 2013 IEEE Topical Conference on Power Amplifiers for Wireless and Radio Applications (PAWR), Austin, TX, USA , 20–20 January 2013; pp. 70–72.
5. Mengozzi, M.; Gibiino, G.P.; Angelotti, A.M.; Santarelli, A.; Florian, C.; Colantonio, P. Automatic Optimization of Input Split and Bias Voltage in Digitally Controlled Dual-Input Doherty RF PAs. *Energies* **2022**, *15*, 4892. [CrossRef]
6. Kantana, C.; Benosman, M.; Ma, R.; Komatsuzaki, Y. A System Approach for Efficiency Enhancement and Linearization Technique of Dual-Input Doherty Power Amplifier. *IEEE J. Microw.* **2023**, *3*, 115–133. [CrossRef]
7. Woo, J.L.; Park, S.; Kim, U.; Kwon, Y. Dynamic stack-controlled CMOS RF power amplifier for wideband envelope tracking. *IEEE Trans. Microw. Theory Tech.* **2014**, *62*, 3452–3464. [CrossRef]
8. Nader, C.; Landin, P.N.; Van Moer, W.; Bjorsell, N.; Handel, P.; Ronnow, D. Peak-Power Controlling Technique for Enhancing Digital Pre-Distortion of RF Power Amplifiers. *IEEE Trans. Microw. Theory Tech.* **2012**, *60*, 3571–3581. [CrossRef]
9. Kim, H.; Seo, C. Improvement of Power Added Efficiency and Linearity in Doherty Amplifier using Dual Bias Control and Photonic Band-Gap Structure. In Proceedings of the 2007 Asia-Pacific Microwave Conference—(APMC 2007), Bangkok, Thailand, 11–14 December 2007; pp. 1–4.
10. Zhu, S.; Chen, X.; Kong, W.; Ding, D.; Xia, J. A harmonic controlled doherty power amplifier with enhanced efficiency at back-off power. In Proceedings of the 2017 Sixth Asia-Pacific Conference on Antennas and Propagation (APCAP), Xi'an, China, 16–19 October 2017; pp. 1–3.
11. Xiao, Z.; Hu, Y.; Wang, W. A Doherty power amplifier employing direct input power dividing technology. In Proceedings of the 2012 International Workshop on Microwave and Millimeter Wave Circuits and System Technology (MMWCST), Chengdu, China, 19–20 April 2012; pp. 1–3.
12. Wincza, K.; Smolarz, R.; Gruszczynski, S. Broadband Differentially-Fed Directional Coupler Composed of Coupled and Uncoupled Sections. In Proceedings of the 2019 IEEE Asia-Pacific Microwave Conference (APMC), Singapore, 10–13 December 2019; pp. 1131–1133.
13. Smolarz, R.; Wincza, K.; Gruszczynski, S. Design of 3-dB Differentially-Fed Tandem Directional Couplers. In Proceedings of the 2019 IEEE MTT-S International Wireless Symposium (IWS), Guangzhou, China, 19–22 May 2019; pp. 1–3.
14. Shuichi, S.; Yuji, K.; Shintaro, S. Adaptive Input-Power Distribution in Doherty Power Amplifier using ModifiedWilkinson Power Divider. In Proceedings of the 2020 IEEE Topical Conference on RF/Microwave Power Amplifiers for Radio and Wireless Applications (PAWR), San Antonio, TX, USA, 26–29 January 2020; pp. 34–37.
15. Lopera, J.R.; Mayock, J.; Sun, Q.; Gadringer, M.; Bosch, W.; Leitgeb, E. A 3.5GHz High Power GaN Hybrid Doherty Power Amplifier with Dynamic Input Power Splitting for Enhanced Power Added Efficiency at Backoff. In Proceedings of the 2021 IEEE Topical Conference on RF/Microwave Power Amplifiers for Radio and Wireless Applications (PAWR), San Diego, CA, USA, 17–20 January 2021; pp. 1–4.
16. Kumari, C.; Chattoraj, N. Design of an Elementary Microstrip Power Splitter for Antenna Array. In Proceedings of the 2021 National Conference on Communications (NCC), Virtual, 27–30 July 2021; pp. 1–5.
17. Masood, M.; Staudinger, J.; Wood, J.; Bokatius, M.; Kenney, J.S. Linearity considerations for a high power Doherty amplifier. In Proceedings of the 2012 IEEE Topical Conference on Power Amplifiers for Wireless and Radio Applications (PAWR), Santa Clara, CA, USA, 15–18 January 2012; pp. 77–80.

18. Hau, G.; Nishimura, T.B.; Iwata, N. A highly efficient linearized wide-band CDMA handset power amplifier based on pre-distortion under various bias conditions. *IEEE Trans. Microw. Theory Tech.* **2001**, *49*, 1194–1201. [CrossRef]

19. Tiwari, T.; Krishnan, R. Design and development of waveguide type dual directional coupler for s-band linear accelerator. In Proceedings of the 2008 International Conference on Recent Advances in Microwave Theory and Applications (MICROWAVE), Jaipur, India, 21–24 November 2008; pp. 252–254.

20. Kim, C.-S.; Lim, J.-S.; Kim, D.-J.; Ahn, D. A design of single and multi-section microstrip directional coupler with the high directivity. In Proceedings of the 2004 IEEE MTT-S International Microwave Symposium Digest, Fort Worth, TX, USA, 6–11 June 2004.

21. Adya, S.; Jain, A.; Sharma, D.; Gupta, A.; Bhalla, V. Design and fabrication of microstrip equal Wilkinson RF power divider at 650MHz using MWO. In Proceedings of the 2017 IEEE Applied Electromagnetics Conference (AEMC), Aurangabad, India, 19–22 December 2017; pp. 1–2.

22. Ahn, S.-H.; Lee, J.W.; Cho, C.S.; Lee, T.K. A Wilkinson Power Divider with Different Power Ratios at Different Frequencies. In Proceedings of the 2007 Asia-Pacific Microwave Conference—(APMC 2007), Bangkok, Thailand, 11–14 December 2007; pp. 1–4.

23. Najib, N.; You, K.Y.; Lee, C.Y.; Dimon, M.N.; Khamis, N.H. Compact and wideband modifiedWilkinson power dividers. In Proceedings of the 2017 IEEE 4th International Conference on Smart Instrumentation, Measurement and Application (ICSIMA), Putrajaya, Malaysia, 28–30 November 2017; pp. 1–4.

24. Jongsuebchoke, I.; Torrungrueng, D.; Akkaraekthalin, P. A graphical study of quarter-wave-like transformers implemented using conjugately characteristic-impedance transmission lines. In Proceedings of the 2016 13th International Conference on Electrical Engineering/Electronics, Computer, Telecommunications and Information Technology (ECTI-CON), Chiang Mai, Thailand, 28 June–1 July 2016; pp. 1–5.

25. Shealy, J.; Smart, J.; Poulton, M.; Sadler, R.; Grider, D.; Gibb, S.; Hosse, B.; Sousa, B.; Halchin, D.; Steel, V.; et al. Gallium nitride (GaN) HEMT's: Progress and potential for commercial applications. In Proceedings of the IEEE Gallium Arsenide Integrated Circuits Symposium, Monterey, CA, USA, 20–23 October 2002; pp. 243–246.

26. Jeong-Sun, M.; Jongchan, K.; Dave, B.; Robert, G.; Danny, W.; Helen, F.; Peter, C.; Dustin, L.; Haw, T.; Chuck, M. 100-MHz–8 GHz linear distributed GaN MMIC power amplifier with improved power-added efficiency. In Proceedings of the 2017 IEEE Topical Conference on RF/Microwave Power Amplifiers for Radio and Wireless Applications (PAWR 2017), Phoenix, AZ, USA, 15–18 January 2017; pp. 40-43.

27. Quaglia, R.; Camarchia, V.; Jiang, T.; Pirola, M.; Guerrieri, S.D.; Loran, B. K-Band GaAs MMIC Doherty Power Amplifier for Microwave Radio With Optimized Driver. *IEEE Trans. Microw. Theory Tech.* **2014**, *62*, 2518–2525. [CrossRef]

28. Nam, J.M.; Ho, J.W.; Rea, C.M.; Hyun, L.Y. Design and realization of driving amplifier MMIC circuit stages for KT IMT-2000 handset. In Proceedings of the IEEE Region 10 Conference. TENCON 99. 'Multimedia Technology for Asia-Pacific Information Infrastructure', Cheju, Republic of Korea, 15–17 September 1999.

29. Li, X.; Fu, H.; Ma, K.; Hu, J. A 2.4–4-GHz Wideband 7-Bit Phase Shifter with Low RMS Phase/Amplitude Error in 0.5-μm GaAs Technology. *IEEE Trans. Microw. Theory Tech.* **2022**, *70*, 1292–1301. [CrossRef]

30. Heismann, F.; Ulrich, R. Integrated-Optical Single-Sideband Modulator and Phase Shifter. *IEEE Trans. Microw. Theory Tech.* **1982**, *30*, 613–617. [CrossRef]

31. Lee, H.-S.; Min, B.-W. W-Band CMOS 4-Bit Phase Shifter for High Power and Phase Compression Points. *IEEE Trans. Circuits Syst. II Express Briefs* **2014**, *62*, 1–5. [CrossRef]

32. Liu, C.; Cheng, Q.-F. Analysis and Design of High-Efficiency Parallel-Circuit Class-E/F Power Amplifier. *IEEE Trans. Microw. Theory Tech.* **2019**, *67*, 2382–2392. [CrossRef]

33. Leng, Y.; Zeng, Y.; Zhang, L.; Zhang, G.; Peng, Y.; Guan, J.; Yan, Y. An Extended Topology of Parallel-Circuit Class-E Power Amplifier Using Transmission-Line Compensation. *IEEE Trans. Microw. Theory Tech.* **2013**, *61*, 1628–1638. [CrossRef]

34. Sah, P.; Kakaraparty, K.; Poulton, M.; Luyen, H.; Mahbub, I. Prototype for an Optimized Drive Signal Control System for a 2.5 GHz Doherty Power Amplifier. In Proceedings of the 2022 IEEE Texas Symposium on Wireless and Microwave Circuits and Systems (WMCS), Waco, TX, USA, 19–20 April 2022; pp. 1–4.

35. Costanzo, F.; Camarchia, V.; Carvalho, N.B.; Colantonio, P.; Piacibello, A.; Quaglia, R.; Valenta, V.; Giofre, R. A GaN MMIC Stacked Doherty Power Amplifier For Space Applications. In Proceedings of the 2022 IEEE Topical Conference on RF/Microwave Power Amplifiers for Radio and Wireless Applications (PAWR), Las Vegas, NV, USA, 16–19 January 2022; pp. 29–31.

36. Shukla, S.; Kitchen, J. GaN-on-Si switched mode RF power amplifiers for non-constant envelope signals. In Proceedings of the 2017 IEEE Topical Conference on RF/Microwave Power Amplifiers for Radio and Wireless Applications (PAWR), Phoenix, AZ, USA, 15–18 January 2017; pp. 88–91.

37. Lin, Q.; Wu, H.-F.; Hua, Y.-N.; Chen, Y.-J.; Hu, L.-L.; Liu, L.-S.; Chen, S.-J. A 2–20-GHz 10-W High-Efficiency GaN Power Amplifier Using Reactive Matching Technique. *IEEE Trans. Microw. Theory Tech.* **2020**, *68*, 3148–3158. [CrossRef]

38. Ćwikliński, M.; Brückner, P.; Leone, S.; Friesicke, C.; Maßler, H.; Lozar, R.; Sandrine, W.; Rüdiger, Q.; Oliver, A. D-Band and G-Band High-Performance GaN Power Amplifier MMICs. *IEEE Trans. Microw. Theory Tech.* **2019**, *67*, 5080–5089. [CrossRef]

39. Piacibello, A.; Quaglia, R.; Camarchia, V.; Ramella, C.; Pirola, M. Dual-input driving strategies for performance enhancement of a doherty power amplifier. In Proceedings of the 2018 IEEE MTT-S International Wireless Symposium (IWS), Chengdu, China, 6–10 May 2018; pp. 1–4.
40. Piacibello, A.; Pirola, M.; Camarchia, V.; Ramella, C.; Quaglia, R.; Zhou, X.; Chan, W.-S. Comparison of S-band Analog and Dual-Input Digital Doherty Power Amplifiers. In Proceedings of the 2018 13th European Microwave Integrated Circuits Conference (EuMIC), Madrid, Spain, 23–25 September 2018.